

Article

Solvent Effects in the Regioselective N-Functionalization of Tautomerizable Heterocycles Catalyzed by Methyl Trifluoromethanesulfonate: A Density Functional Theory Study with Implicit Solvent Model

Nelson H. Morgon ¹, Srijit Biswas ², Surajit Duari ² and Aguinaldo R. de Souza ^{3,*}

¹ Department of Physical Chemistry, Institute of Chemistry, Campinas State University, Campinas 13083-970, São Paulo, Brazil

² Department of Chemistry, University of Calcuta, 92, A.P.C. Road, Kolkata 700 009, West Bengal, India

³ Department of Chemistry, School of Science, São Paulo State University, Bauru 17033-360, São Paulo, Brazil

* Correspondence: aguinaldo.robinson@unesp.br

Abstract: Methyl trifluoromethanesulfonate was found to catalyze the reaction of the nucleophilic substitution of the hydroxyl group of alcohols by *N*-heterocycles followed by *X*- to *N*-alkyl group migration (*X* = O, S) to obtain *N*-functionalized benzoxazolone, benzothiazolethione, indoline, benzoimidazolethione and pyridinone derivatives. A high degree of solvent dependency on the yield of the products was observed during optimization of the reaction parameters. The yield of the product was found to be 0%, 48% and 70% in acetonitrile, 1,2-dichloroethane and chloroform, respectively. The mechanism of the reaction was established through experiments as well as DFT calculations. The functional B3LYP and 6-311++G(d) basis function sets were used to optimize the molecular geometries. D3 Grimme empiric dispersion with Becke–Johnson damping was employed, and harmonic vibrational frequencies were calculated to characterize the stationary points on the potential energy surface. To ensure that all the stationary points were smoothly connected to each other, intrinsic reaction coordinate (IRC) analyses were performed. The influence of solvents was considered using the solvation model based on density (SMD). The free energy profiles of the mechanisms were obtained with vibrational unscaled zero-point vibrational energy (ZPE), thermal, enthalpy, entropic and solvent corrections.

Keywords: methyl trifluoromethanesulfonate; solvent effects; density functional theory; potential energy surface



Citation: Morgon, N.H.; Biswas, S.; Duari, S.; de Souza, A.R. Solvent Effects in the Regioselective N-Functionalization of Tautomerizable Heterocycles Catalyzed by Methyl Trifluoromethanesulfonate: A Density Functional Theory Study with Implicit Solvent Model. *Computation* **2022**, *10*, 172. <https://doi.org/10.3390/computation10100172>

Academic Editor: Alexander S. Novikov

Received: 17 August 2022

Accepted: 21 September 2022

Published: 26 September 2022

Publisher's Note: MDPI stays neutral with regard to jurisdictional claims in published maps and institutional affiliations.



Copyright: © 2022 by the authors. Licensee MDPI, Basel, Switzerland. This article is an open access article distributed under the terms and conditions of the Creative Commons Attribution (CC BY) license (<https://creativecommons.org/licenses/by/4.0/>).

1. Introduction

Nucleophilic bimolecular chemical reactions play a great role in chemistry and biochemistry and are valuable tools to construct functional groups. Chemical reactions are sensitive to the presence of the surrounding solvent, and the free energy profiles in the gas phase are significantly different when in solution. The free energy profile is one of the most important quantities to unravel the solvent effect on the reaction mechanism and reaction dynamics. The presence of solvent can alter the free energy profile along the reaction coordinates and modify the presence of minima and the energy barriers between reactants and products [1].

The Menshutkin reaction is a special kind of S_N2 reaction where the reactants are uncharged, and it was found that the reaction rate increases with the polarity of the solvent. For polar solvents such as water, methanol, acetonitrile and benzene, strong solvent effects were found, whereas for apolar and cyclohexane, there is no pronounced barrier reduction. As the system approaches the TS, correlated solvent motions occur, destabilizing the solvent–solute interactions [2]. From the analysis of this reaction, the

solvent effects were classified into two main categories: static and dynamic. In the static regime, the solvent molecules are equilibrated for each given geometry of the solute in a passive role in the chemical reaction. On the other hand, solvents' effects are more pronounced in a nonequilibrium state. The extents of equilibration of the solvent were governed by the strength of the solvent–solute interactions and modifications in the free energy profile [3].

Recent studies proposed a multiscale reaction density functional theory (RxDFT) by combining quantum and classical DFT in the calculation of the intrinsic free energy to account for the solvation free energy [4]. This methodology was applied to obtain the free energy profiles of the tautomerization of the amino acid glycine in an aqueous solution. Barrier height reductions was observed in moving from the gas phase to polar solvents, and the solvent distributions change between reactant, transition state and product, reflected in the solvent–solvent interactions. MP2 and DFT calculations were performed in the study of basis set extrapolation and solvent effects in CO₂ sequestration reactions with anions [5]. Both methodologies were similar for the reaction's thermodynamics, and the reactions in the gas phase are highly exothermic and do not involve any activation barrier. The results obtained with the solvent tetrahydrofuran are in closer agreement with water and toluene, and for some anions, the authors observed a change in the reaction spontaneity in the different solvents. Most reactions do not show a transition state, either in the gas or solution phase.

Although previous studies have shed some light upon the thermodynamics and free energy profile of chemical reactions as a function of the solvent, many questions still remain, such as the effect of the solvent on the yield of regioselective functionalization reactions. In the study of the regioselection switch in nucleophilic addition to isoquinolinequinones, the mechanism obtained in the total synthesis of ellipticine required explicit solvent molecules [6]. Porto et al. observed, in the investigation of the cooperative effect of solvents, that not only hybrid solvation may be required, but also the number of explicit molecules added may heavily influence the calculated reaction rates [7].

The demand for new antibiotics within a wide range is a global challenge for the academic as well for the pharmaceutical industry. Some organic molecules having benzoxazole, benzothiazole and related structural motifs have been reported to have antitumor, antiviral, anti-inflammatory and antimicrobial activities [8,9]. The regioselective functionalization of the N-center of tautomerizable benzoxazole, benzothiazole, is an atom-efficient method to produce a new class of antibiotics. The yield of the functionalization, using commercially available Brønsted acids such as trifluoromethanesulfonic acid (TfOH), is solvent-dependent. The yield is equal to 80, 70, 48, 20, 0 and 23% in toluene, chloroform, dichloroethane, diisopropyl ether, acetonitrile and nitromethane, respectively [10]. To gain a further understanding of the solvent effects on the role of methyl trifluoromethanesulfonate (MeOTf), DFT calculations were performed through the study of the potential energy surface involving the cooperative effects of MeOTf for the formation of the products.

2. Computational Methodology

Density functional theory (DFT) calculations were performed using the Gaussian16 suite of programs [11]. The molecular geometries of the species **1a**, **2a**, MeOTf, Int1 (2a-OMe), TfOH, Int2, MeOH, TfOH, Int3, H₂O and **3a**, presented in Table 1 of Duari et al. [8], were carried out using the B3LYP functional devised by Becke [12]. The B3LYP functional uses the LYP expression for both local and non-local terms, and the VWN functional III for local correlation. The Pople basis set 6-311++G(2d,p) was used for all systems due to its large size, and s-functions and a set of diffuse functions have been added to each heavy atom [13,14]. The Grimme's empirical implementation GD3(BJ) adds empirical dispersion corrections to the B3LYP functional, and the performance with the basis sets was found to be outstanding among a variety of functionals in previous studies [15].

Table 1. Imaginary frequencies (cm^{-1}), dielectric constant (in Debye) and yield (%) of the reactions associated with the transition states as a function of the solvent.

Solvent	Imaginary Frequency	Dielectric Constant	Yield
TOL	127.27i	2.37	80
DIP	132.64i	3.38	20
CHL	68.21i	4.71	70
DCE	48.83i	10.13	48
CAN	-	35.69	0
NIT	-	36.56	23

Solvents were modeled using the continuum solvation model, SMD, where “D” stands for density to denote that the full solute electron density is used without the need to define the partial atomic charges. The molecules of the solvent were represented implicitly as a dielectric medium, with a surface tension at the solute–solvent boundary. The SMD solvation model is applicable to a charged or neutral solute in any solvent and separates the observable solvation free energy into the bulk electrostatic contribution arising from the self-consistent reaction field (SCRf) treatment, and the interactions arising from short-range interactions between the solute and solvent molecules in the first solvation layer. The SMD model was parametrized with a set of 2821 solvation data, including 112 aqueous ionic media’s solvation free energy, solvation free energies for ions in acetonitrile, methanol and dimethyl sulfoxide, solvation free energy for neutral solutes in 91 solvents and transfer free energy for 93 neutral solutes in 15 solvents including water.

The SMD model uses a single set of parameters called intrinsic atomic Coulomb radii and atomic surface tension coefficients, optimized over six electronic structure methods. Along with the 6–31G* basis set family, the SMD model presents a mean error of 0.6–1.0 kcal/mol in the solvation free energies for neutral solutes and errors of 4 kcal/mol for ions [16]. Other possible solvent effects, such as hydrogen bonds, are not considered using the SMD approach. Another possibility is the inclusion of explicit solvent molecules in a hybrid implicit–explicit solvation schema. This approach has difficulty in defining the number and location of explicit solvent molecules, and the conformational space strongly increases, making necessary the use of extensive conformational sampling. The choice of a continuum schema against an explicit model in the present work will be a contribution to setting the limits of this model in a reactive system. The investigated solvents, in crescent order of the dielectric constant, were toluene (TOL), diisopropylether (DIP), chloroform (CHL), dichloroethane (DCE), acetonitrile (CAN) and nitromethane (NIT), as this is the parameter that the SMD model uses for solvent polarity.

Single-point frequency calculations were done to ensure that the optimized structures, reactants and products could be obtained without imaginary frequency modes or, in the case of the transition state, only one imaginary frequency. The transition states for the reactions in all solvents were identified by performing intrinsic reaction coordinate (IRC) calculations at the B3LYP-GD3(BJ)/6-311++G(3df,2p)+SMD(Solvent) level of theory, basis sets and solvation model, respectively. To characterize the reaction mechanism, the following electronic properties were calculated: electronic chemical potential (μ), chemical hardness (η), electrophilicity (ω) and nucleophilicity (N). They were calculated at the B3LYP+GD3(BJ)/6-311++G(3df,2p) level of theory in diisopropylether solvent using the SMD model of solvation.

3. Results and Discussion

To study the solvent effects on the regioselective functionalization of the N-center of tautomerizable benzoxazole, we proceed to the calculation of the imaginary frequencies. These frequencies are associated with the transfer between the -R group in the R-O-C and N-C bond. The corresponding transition state properties are given in Table 1.

The reaction yield decreases with the increase in solvent polarity, but in some cases, such as diisopropylether and nitromethane, the reaction yield was very similar, although the difference in the dielectric constant was considerable. For those solvents where the transition state was not observed, as for acetonitrile and nitromethane, the yield was equal to 0 and 23, respectively. The yields for non-polar solvents, toluene, diisopropylether, chloroform and dichloroethane, are very compatible with the findings with the SMD model of solvation.

The polar solvent acetonitrile does not present an imaginary frequency associated with the transition state, in good agreement with the experimental reaction yield equal to zero, but the nitromethane solvent does not present an imaginary frequency either, which is in poor agreement with the reaction yield of 23%. The SMD model of solvation was not able to describe the solvent effect in the case of acetonitrile and nitromethane, where the polarity is not the only characteristic to take into account. For these cases, a hybrid implicit–explicit model of solvation is necessary.

A further analysis was done to unravel the possibility of the SMD model of solvation to take into account the solvents' effects in the regioselective functionalization of the N-center of tautomerizable benzoxazole, the intrinsic reaction coordinate (IRC) approach.

In the IRC analysis, the reaction path was followed by integrating the intrinsic reaction coordinate [17,18]. The transition state is the initial geometry, and the path was followed in both directions from these points. The forward direction was defined as the direction that the transition vector was pointing when the largest component of the phase was positive. The reaction mechanism was followed in both directions, forward and reversed. The IRC analysis is presented in Figure 1 for the solvents toluene, chloroform and diisopropylether.

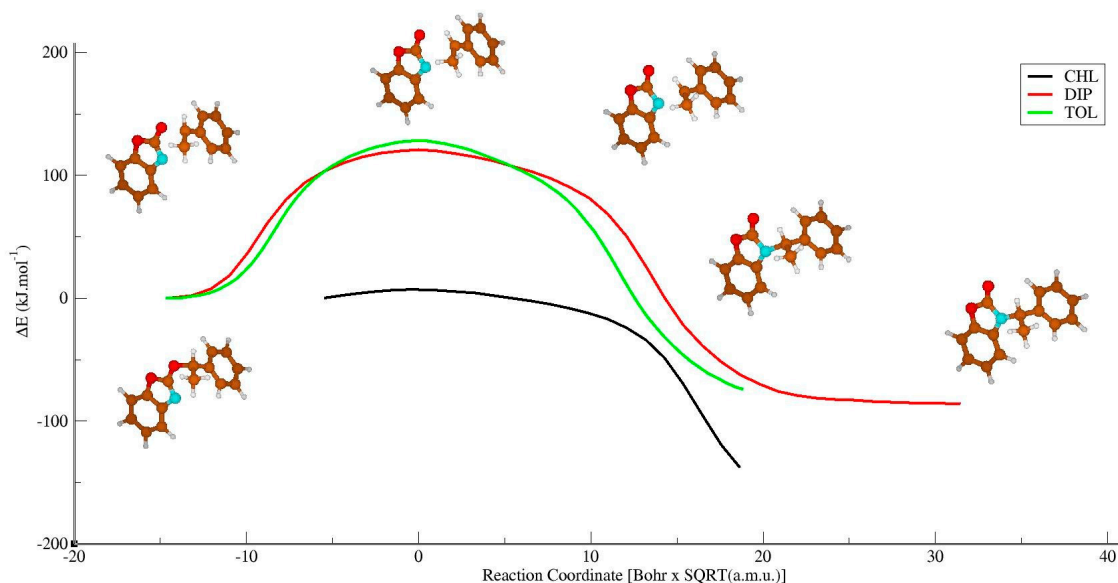


Figure 1. IRC analysis for the solvents toluene, chloroform and diisopropylether.

The transition state energies in toluene and diisopropylether are very similar, in poor agreement with the yield reaction of 20 and 80%, respectively. In the case of toluene, the SMD model is in good agreement with the yield obtained experimentally, 70%, indicating that, for this solvent, the implicit model can account for the solvent effects. A possible explanation for the failure of the SMD model of solvation (or its implicit character) can be the proximity of the static and optical dielectric constant of the solvents diisopropylether and chloroform, as shown in Table 2.

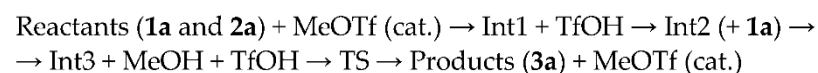
Table 2. Static and optical dielectric constants ^(a) of the solvents used in the present work.

	ACN	CHL	DCE	DIP	NIT	TOL
EPS	35.6880	4.7113	10.1250	3.3800	36.5620	2.3741
EPSINF	1.8069	2.0906	2.0874	1.8712	1.9091	2.2383

^(a) EPS and EPSINF describe static and optical dielectric constants, respectively.

The SMD model is unable to quantitatively distinguish barriers associated with activation energies. It is only observed the formation of transition states, higher absolute values of the imaginary frequencies and characteristic IRCs associated with the normal mode of vibration connecting the intermediates Int2 and Int3 and leading to the formation of product (3a), as presented in Schema 1. These results correspond to the lowest values of static dielectric constants (EPS).

Scheme 1 shows the reactional process between species 1a and 2a catalyzed by MeOTf, leading to the formation of the intermediaries Int1, Int2, Int3, TS and the products (3a). From the experimental point of view, to optimize the reaction parameters, benzo[d]oxazol-2-ol (1a) and 1-phenylethan-1-ol (2a) were considered as the model for the nucleophilic and electrophilic partners, respectively, and the formation of the N-substituted benzoxazolones species, 3a, was monitored.



Scheme 1. Scheme 1 shows the reactional process between species 1a and 2a catalyzed by MeOTf, leading to the formation of the intermediaries Int1, Int2, Int3, TS and the products (3a).

Scheme 1 was studied from the index of electrophilicity and nucleophilicity concept of the different species presented in the mechanism of the reaction [19–21]. The electrophilicity index represents the stabilizing energy that a molecule receives when it acquires enough electrons to be saturated. It is a measure of its ability to accommodate extra electrons. Both the index (ω) and nucleophilicity index (N) are calculated using Equations (1) and (2) [22,23].

$$\omega = (\mu^2/2\eta) \quad (1)$$

$$N = E_{\text{HOMO(Nu)}} (\text{eV}) - E_{\text{LUMO(TCE)}} (\text{eV}) \quad (2)$$

where μ is equal to the chemical potential, η the global hardness, and HOMO is the highest occupied molecular orbital, and LUMO the lowest unoccupied molecular orbital. The 1a species presents a nitrogen atom with a Parr electrophilicity and nucleophilicity equal to 0.106 and -0.244 , respectively, while the 2a species (both the reactants) presents a 7C center, bounded to a hydroxyl group, with an electrophilicity and nucleophilicity equal to -0.022 and -1.898 , respectively (Figure 2). These two centers will participate in the formation of the intermediary Int1, presented in Figure 3.

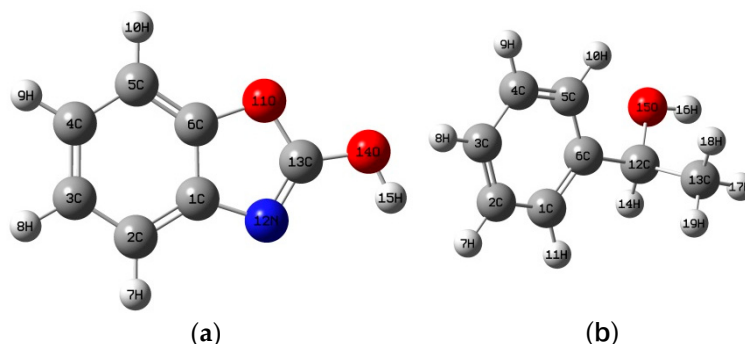


Figure 2. Species (a,b) of Scheme 1.

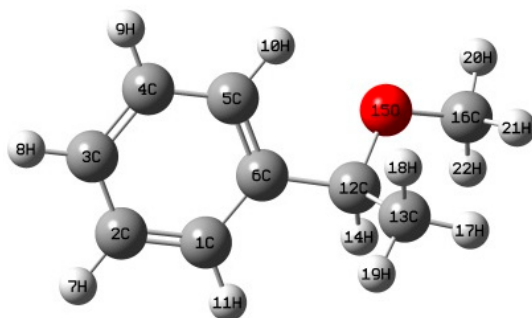


Figure 3. Parr index for the oxygen atom at Int1.

The intermediary Int1 has an oxygen atom center with electrophilicity and nucleophilicity equal to 0.120 and 0.002, respectively. This change in the Parr index is due to the formation of the chemical bond between the species **1a** and **2a** and shows higher electrophilicity.

The next intermediary, Int2, presents a 1O center with electrophilicity and nucleophilicity equal to 0.021 and 0.007, respectively. These values are lower than that presented by the same atom in Int1, leading to the formation of a hydrogen bond between the 1O atom and 2O of the species TfOH (Figure 4).

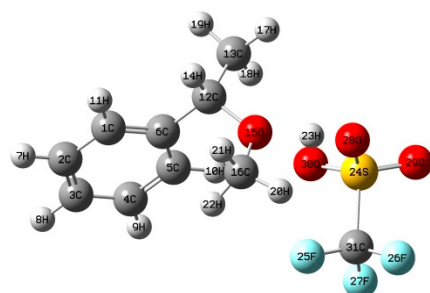


Figure 4. Formation of a hydrogen bond in Int2 between the species Int1 and TfOH.

In the next step of the chemical reaction, we have the formation of the species Int3 that presents a nitrogen atom center with an electrophilicity and nucleophilicity equal to 0.133 and -0.025 , respectively (Figure 5). This center has higher electrophilicity than the previous nitrogen center at species **1a** and can participate in electrophilic chemical reactions. This species in the presence of MeOH and TfOH leads to the formation of the transition state, as shown in Figure 6.

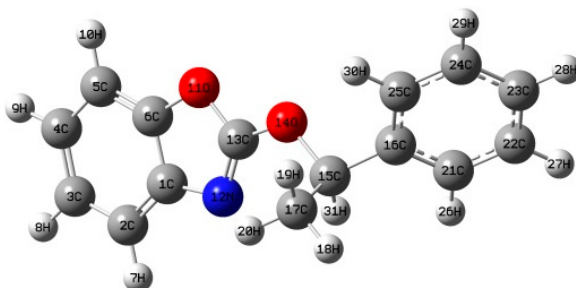


Figure 5. Int3 species with higher electrophilicity of the nitrogen atom center.

The transition state presents an 8C center with an electrophilicity and nucleophilicity equal to -0.013 and 0.695, respectively, and an N center with an electrophilicity and nucleophilicity equal to 0.314 and 0.004, respectively. The presence of these two centers, with higher nucleophilicity and electrophilicity, leads to the formation of the species **3a** in accordance with the experimental results.

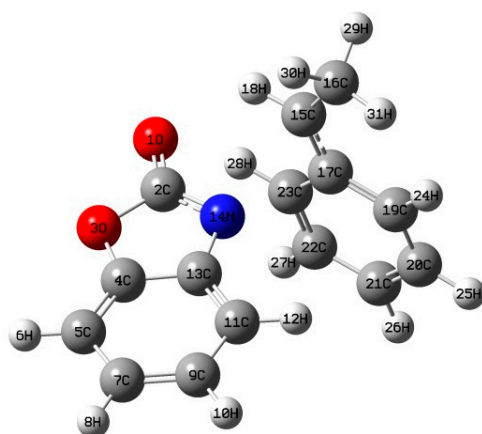


Figure 6. Transition state formed from the species Int3.

Figure 7 shows the calculated Gibbs free energy profile and the mechanisms involving the cooperative catalytic effects of MeOTf compared to TfOH using solvents toluene and diisopropylether. The red and blue lines are related to the mechanism in the diisopropylether and toluene solvent, respectively. As can be seen, the higher value of the activation of toluene, in relation to diisopropylether, is in poor concordance with the experimental results. The experimental yield of the reaction is greater in toluene (80%) in relation to diisopropylether (20%), showing that the SMD model of solvation is not adequate to take into account all the solvent effects in the studied reactions. It is possible that a hybrid explicit-implicit model for the solvation can take into account other kinds of interactions, such as hydrogen bonds between the solute and solvent, and other non-covalent interactions.

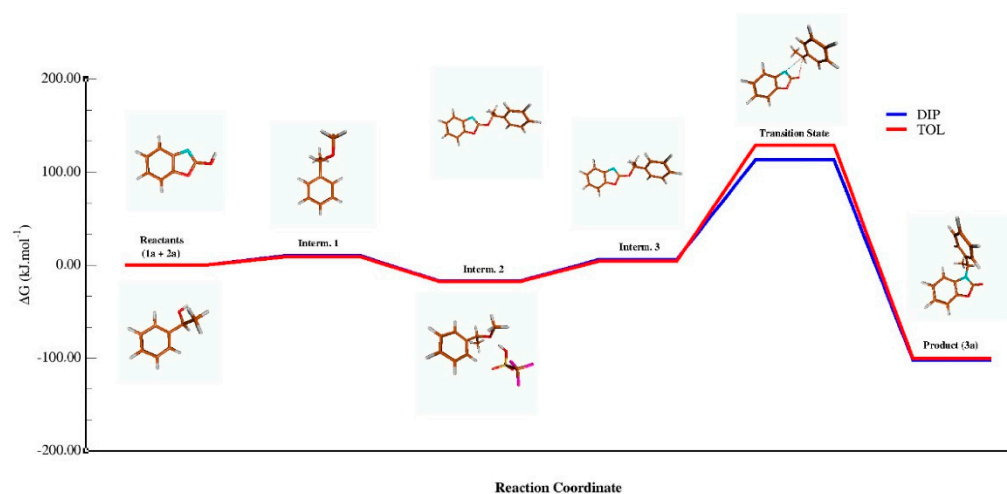


Figure 7. Potential energy surface involving the cooperative catalytic effects of MeOTf compared to TfOH using solvents toluene and diisopropylether.

4. Conclusions

In this work, we evaluate, through DFT calculations, the reaction mechanism of the regioselective N-functionalization of tautomerizable heterocycles catalyzed by MeOTf in different solvents. The study of the reaction mechanism took place through the construction of the potential surface energy, as well as the electronic properties, such as chemical potential, chemical hardness and electro- and nucleophilicity. Implicit solvation models are unable to distinguish the yields observed experimentally, especially when there is great similarity in the parameters that define these solvents. Although diisopropylether has a lower yield than the toluene solvent (20 and 80%, respectively), the reaction coordinate profile and the IRCs associated with the transition states that determine the proposed mechanism are very similar.

Studies describing the solvent effect through a hybrid model (SCRF and solvent molecules) may have potential to advance the understanding of this reaction both from a qualitative and quantitative point of view. In addition to hybrid models of solvation, where solvent molecules are treated explicitly while considering solvent long-range effects as implicit, the full simulation of solvent effects is possible using density functional-based ab initio molecular dynamics techniques, where the emphasis is on the dynamical aspects of the reaction mechanism in both the molecular and condensed phase.

The methodology used in this work, based on the B3LYP functional, underestimates the energy barrier heights of the reaction mechanism. More accurate CCSD(T) methods could be used, where the inclusion of triple excitations is necessary for achieving satisfactory accuracy. Further investigations using the CCSD(T) methodology are in progress to describe the solvent effects on the yields of regioselective functionalization reactions.

Author Contributions: Conceptualization, S.B., S.D., N.H.M. and A.R.d.S.; methodology, N.H.M. and A.R.d.S.; validation, S.B., S.D., N.H.M. and A.R.d.S.; formal analysis, S.B., S.D., N.H.M. and A.R.d.S.; investigation, S.B., S.D., N.H.M. and A.R.d.S.; resources, N.H.M.; data curation, N.H.M. and A.R.d.S.; writing—original draft preparation, S.B., S.D., N.H.M. and A.R.d.S.; funding acquisition, N.H.M. and A.R.d.S. All authors have read and agreed to the published version of the manuscript.

Funding: FAPESP (19/12294-5, 15/22338-9), CNPq, CAPES.

Data Availability Statement: Computational data for this research are freely available.

Acknowledgments: The authors are grateful for the support from the Department of Physical Chemistry, Institute of Chemistry, Campinas State University, Campinas, São Paulo, Brazil; the Faculty of Science, São Paulo State University, Brazil; the Center for Computing in Engineering & Sciences, UNICAMP; the University Grants Commission (UGC), Govt. of India, for a start-up grant through the FRP program (F.4-5(80-FRP)(IV-Cycle)/2017(BSR); and the Govt. of India for their fellowships.

Conflicts of Interest: The authors declare no conflict of interest.

References

1. Tapia, O.; Bertrán, J. *Solvent Effects and Chemical Reactivity*; Kluwer Academic Publishers: Dordrecht, Holland, 2000; pp. 1–377.
2. Turan, H.T.; Brickel, S.; Meuwly, M. Solvent Effects on the Menshutkin Reaction. *J. Phys. Chem. B* **2022**, *126*, 1951–1961. [[CrossRef](#)]
3. Solà, M.; Lledós, A.; Duran, M.; Bertran, J.; Abboud, J.L.M. Analysis of Solvent Effects on the Menshutkin Reaction. *J. Am. Chem. Soc.* **1991**, *113*, 2873–2879. [[CrossRef](#)]
4. Tang, W.; Zhao, J.; Jiang, P.; Xu, X.; Zhao, S.; Tong, Z. Solvent Effects on the Symmetric and Asymmetric SN2 Reactions in the Acetonitrile Solution: A Reaction Density Functional Theory Study. *J. Phys. Chem. B* **2020**, *124*, 3114–3122. [[CrossRef](#)] [[PubMed](#)]
5. Quattrociochi, D.G.S.; de Oliveira, A.R.; Carneiro, J.W.M.; Rocha, C.M.R.; Varandas, A.J.C. MP2 versus Density functional Theory calculations in CO₂-sequestration reactions with anions: Basis set extrapolation and solvent effects. *Int. J. Quantum Chem.* **2021**, *121*, 126583. [[CrossRef](#)]
6. Castro, J.A.M.; Serikava, B.K.; Maior, C.R.S.; Naciuk, F.F.; Rocco, S.A.; Ligiéro, C.B.P.; Morgon, N.H.; Miranda, P.C.M.L. Regioselection Switch in Nucleophilic Addition to Isoquinolinequinones: Mechanism and Origin of the Regioselectivity in the Total Synthesis of Ellipticine. *J. Org. Chem.* **2022**, *87*, 7610–7617. [[CrossRef](#)] [[PubMed](#)]
7. Porto, C.M.; Santana, L.C.; Morgon, N.H. Theoretical investigation of the cooperative effect of solvent: A case study. *Phys. Chem. Chem. Phys.* **2022**, *24*, 14603–14615. [[CrossRef](#)] [[PubMed](#)]
8. Zhang, W.; Liu, J.; Macho, J.M.; Jiang, X.; Xie, D.; Jiang, F.; Liu, W.; Fu, L. Design, synthesis and antimicrobial evaluation of novel benzoxazole derivatives. *Eur. J. Med. Chem.* **2017**, *126*, 7–14. [[CrossRef](#)] [[PubMed](#)]
9. Seth, K.; Garg, S.K.; Kumar, R.; Purohit, P.; Meena, V.S.; Goyal, R.; Banerjee, U.C.; Chakraborti, A.K. 2-(2-Arylphenyl)benzoxazole as a Novel Anti-Inflammatory Scaffold: Synthesis and Biological Evaluation. *ACS Med. Chem. Lett.* **2014**, *5*, 512–516. [[CrossRef](#)] [[PubMed](#)]
10. Duari, S.; Biswas, S.; Roy, A.; Maity, S.; Mishra, A.; Souza, A.R.; Elsharif, A.; Morgon, N.H.; Biswas, S. Regioselective N-Functionalization of Tautomerizable Heterocycles through Methyl Trifluoromethanesulfonate Catalyzed Substitution of Alcohols and Alkyl Group Migrations. *Adv. Synth. Catal.* **2022**, *365*, 865–872. [[CrossRef](#)]
11. Frisch, M.J.; Trucks, G.W.; Schlegel, H.B.; Scuseria, G.E.; Robb, M.A.; Cheeseman, J.R.; Scalmani, G.; Barone, V.; Mennucci, B.; Petersson, G.A.; et al. *Gaussian 09*; Gaussian, Inc.: Wallingford, CT, USA, 2009.
12. Becke, A.D. Density-functional thermochemistry. III. The role of exact exchange. *J. Chem. Phys.* **1993**, *98*, 5648–5652. [[CrossRef](#)]
13. Binkley, J.S.; Pople, J.A.; Hehre, W.J. Self-consistent molecular orbital methods. 21. Small split-valence basis sets for first-row elements. *J. Am. Chem. Soc.* **1980**, *102*, 939–947. [[CrossRef](#)]

14. Gordon, M.S.; Binkley, J.S.; Pople, J.A.; Pietro, W.J.; Hehre, W.J. Self-consistent molecular-orbital methods. 22. Small split-valence basis sets for second-row elements. *J. Am. Chem. Soc.* **1982**, *104*, 2797–2803. [[CrossRef](#)]
15. Kosar, N.; Ayub, K.; Gilani, M.A.; Muhammad, S.; Mahmood, T. Benchmark Density Functional Theory Approach for the Calculation of Bond Dissociation Energies of the M–O₂ Bond: A Key Step in Water Splitting Reactions. *ACS Omega* **2022**, *7*, 20800–20808. [[CrossRef](#)] [[PubMed](#)]
16. Marenich, A.V.; Cramer, C.J.; Truhlar, D.G. Universal Solvation Model Based on Solute Electron Density and on a Continuum Model of the Solvent Defined by the Bulk Dielectric Constant and Atomic Surface Tensions. *J. Phys. Chem. B* **2009**, *113*, 6378–6396. [[CrossRef](#)] [[PubMed](#)]
17. Fukui, K. The path of chemical-reactions—The IRC approach. *Acc. Chem. Res.* **1981**, *14*, 363–368. [[CrossRef](#)]
18. Hratchian, H.P.; Schlegel, H.B. *Theory and Applications of Computational Chemistry: The First 40 Years*; Dykstra, C.E., Frenking, G., Kim, K.S., Scuseria, G., Eds.; Elsevier: Amsterdam, The Netherlands, 2005; pp. 195–249.
19. Parr, R.G.; Pearson, R.G. Absolute Hardness: Companion Parameter to Absolute Electronegativity. *J. Am. Chem. Soc.* **1983**, *105*, 7512–7516. [[CrossRef](#)]
20. Parr, R.C.; Yang, W. *Density Functional Theory of Atoms and Molecules*; Oxford University Press: New York, NY, USA, 1989.
21. Toro-Labbé, A. Characterization of chemical reactions from the profiles of energy, chemical potential, and hardness. *J. Phys. Chem. A* **1999**, *103*, 4398–4403. [[CrossRef](#)]
22. Parr, R.G.; Szentpály, L.V.; Liu, S. Electrophilicity index. *J. Am. Chem. Soc.* **1999**, *121*, 1922–1924. [[CrossRef](#)]
23. Domingo, L.R.; Chamorro, E.; Pérez, P. Understanding the reactivity of captodative ethylenes in polar cycloaddition reactions. A theoretical study. *J. Org. Chem.* **2008**, *73*, 4615–4624. [[CrossRef](#)] [[PubMed](#)]